Supplemental Materials

Quantifying nucleation *in vivo* reveals the physical basis of prion-like phase behavior

Tarique Khan, Tejbir S. Kandola, Jianzheng Wu, Shriram Venkatesan, Ellen Ketter,
Jeffrey J. Lange, Alejandro Rodríguez Gama, Andrew Box, Jay R. Unruh, Malcolm Cook, and Randal Halfmann

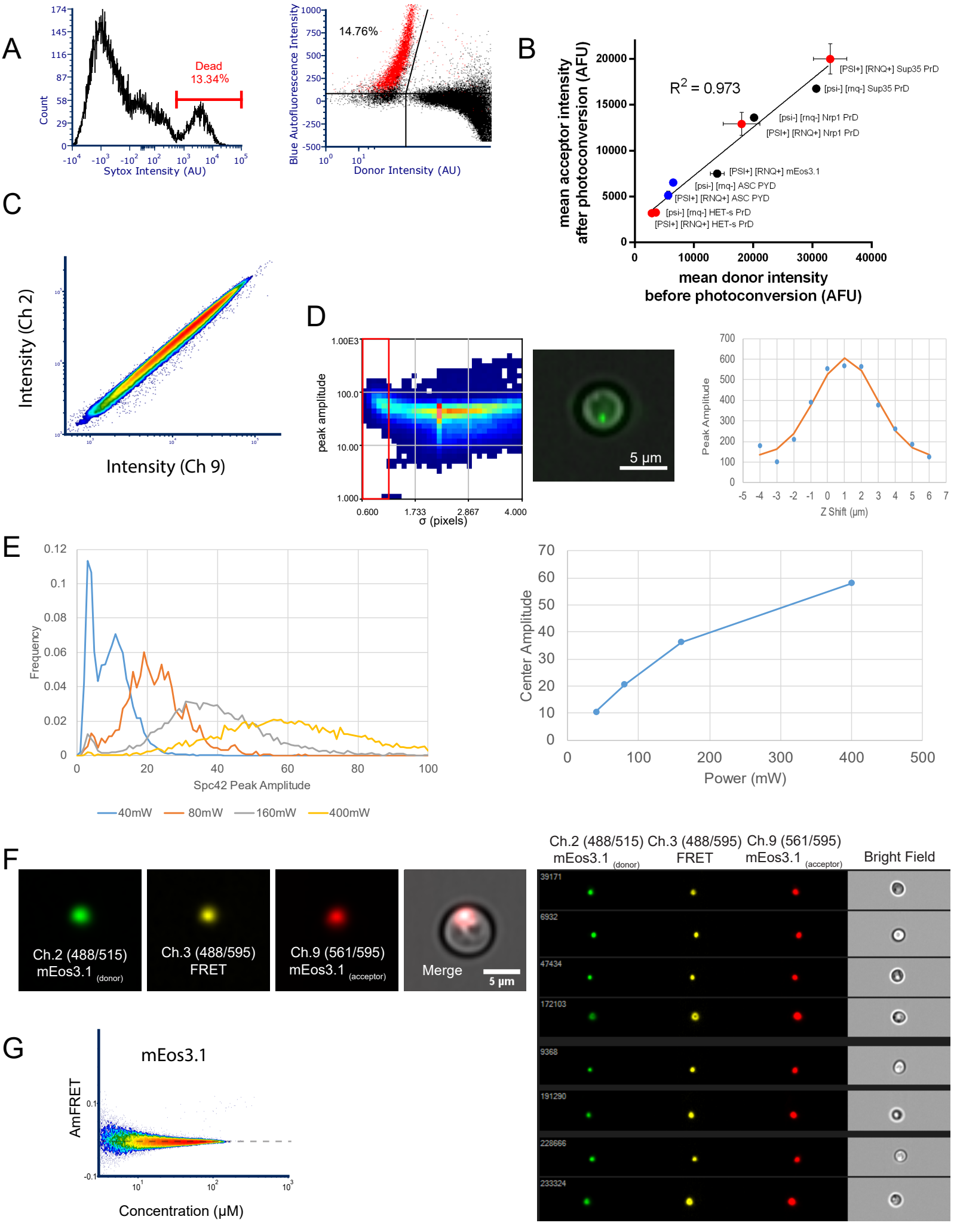
A
Dead
13.34%
Count
Sytox Intensity (AU)
14.76%
Blue Autofluorescence Intensity
Donor Intensity (AU)
B
R2 = 0.973
[PSI+] [RNQ+] Sup35 PrD
[psi-] [rnq-] Sup35 PrD
[psi-] [rnq-] Nrp1 PrD
[PSI+] [RNQ+] Nrp1 PrD
[PSI+] [RNQ+] mEos3.1
[psi-] [rnq-] ASC PYD
[PSI+] [RNQ+] ASC PYD
[psi-] [rnq-] HET-s PrD
[PSI+] [RNQ+] HET-s PrD
mean acceptor intensity after photoconversion (AFU)
mean donor intensity before photoconversion (AFU)
C
Intensity (Ch 2)
Intensity (Ch 9)
D
peak amplitude
σ (pixels)
5 µm
Peak Amplitude
Z Shift (µm)
E
Frequency
Spc42 Peak Amplitude
40mW
80mW
160mW
400mW
Center Amplitude
Power (mW)
F
Ch.2 (488/515) mEos3.1 (donor)
Ch.3 (488/595) FRET
Ch.9 (561/595) mEos3.1 (acceptor)
Merge
5 µm
Ch.2 (488/515) mEos3.1 (donor)
Ch.3 (488/595) FRET
Ch.9 (561/595) mEos3.1 (acceptor)
Bright Field
39171
6932
47434
172103
9368
191290
228666
233324
G
mEos3.1
AmFRET
Concentration (µM)

Figure S1. Technical details and controls for DAmFRET, related to Fig. 1.

(A) Autofluorescence accurately distinguishes live from dead cells. Yeast cells expressing mEos3.1 (not photoconverted) were stained with Sytox Far Red. A histogram of Sytox intensity for single cells is shown on the left, and the Sytox-positive population ("dead") is colored red in the dot plot of blue autofluorescence (405 nm excitation, 457/45 nm emission) vs. mEos3.1 (donor) intensity on the right. Based on this relationship, DAmFRET experiments excluded the population with blue autofluorescence and lacking detectable mEos3.1 fluorescence.
(B) The indicated proteins were expressed in isogenic [psi-] [pin-] or [PSI+] [PIN+] strains and tested for donor intensity prior to photoconversion and then for acceptor intensity following photoconversion. Samples containing amyloid are indicated in red; non-amyloid structured assemblies in blue; and unstructured or monomer in black. The linear regression ($R^2 = 0.9728$) indicates that mEos3.1 photoconversion is independent of fusion, expression level, or structure of the mEos3.1-tagged query protein.
(C) Density plot showing tight correlation of donor and acceptor fluorescence of mEos3.1 following the photoconversion step.
(D) Left-right: A sample image of Spc42-mEos3.1 from the ImageStream®x MkII, a 2D density histogram showing the relationship between Spc42 spot size and peak amplitude showing the selected population for analysis, and a plot of the peak amplitude of beads on the ImageStream as a function of objective focus Z Shift showing the shape of the focal volume (See Methods).
(E) Left: histograms of Spc42-mEos3.1 peak amplitude at different laser powers and Right: the trend of the centers of these histogram peaks (See Methods).
(F) Representative images of High-FRET cells from DAmFRET data of ASC. The panels are (left to right) donor, FRET, acceptor, and bright field merged with acceptor signal.
(G) DAmFRET plot of cells expressing mEos3.1 without a fusion partner.

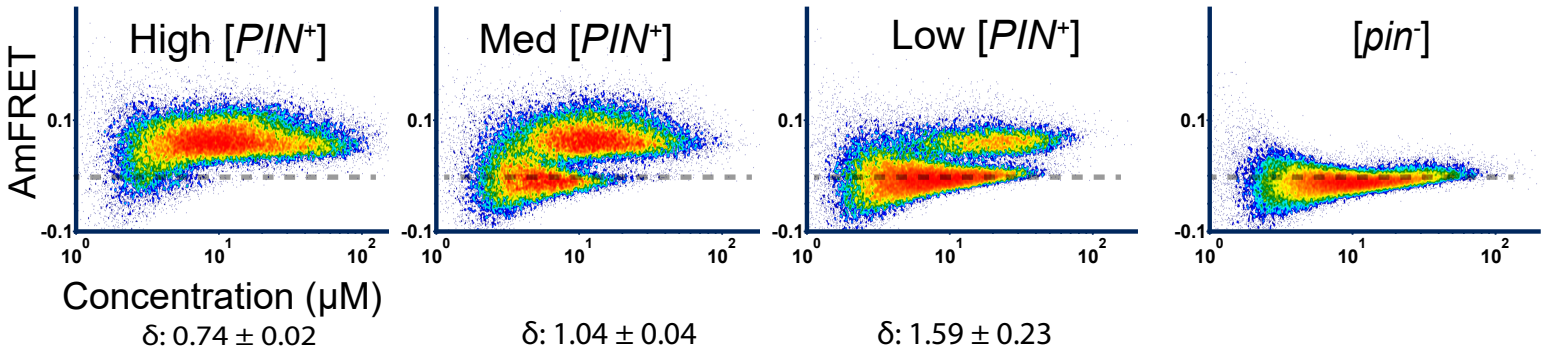

Figure S2. Corresponding DAmFRET plots of the curve fits shown in Fig. 2D, related to Fig. 2. (left to right) DAmFRET plots of Sup35 PrD in cells containing decreasing strengths of the heterotypic nucleator [*PIN*$^+$] showing increasing concentration dependence.


A
Ch2
Donor
Ch3
FRET
Ch9
Acceptor
Ch10
BF
Sup35 PrD
High
Sup35 PrD
Low
Rnq1
High
Rnq1
Low
Cyc8 PrD
High
Cyc8 PrD
Low

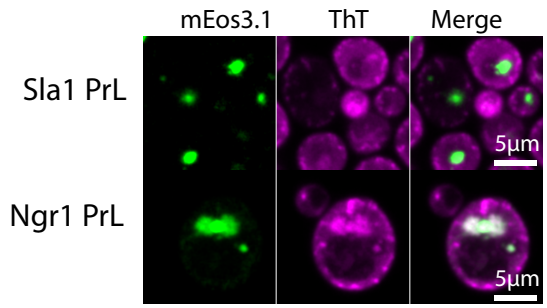
B
mEos3.1
ThT
Merge
Sla1 PrL
Ngr1 PrL
5μm
5μm

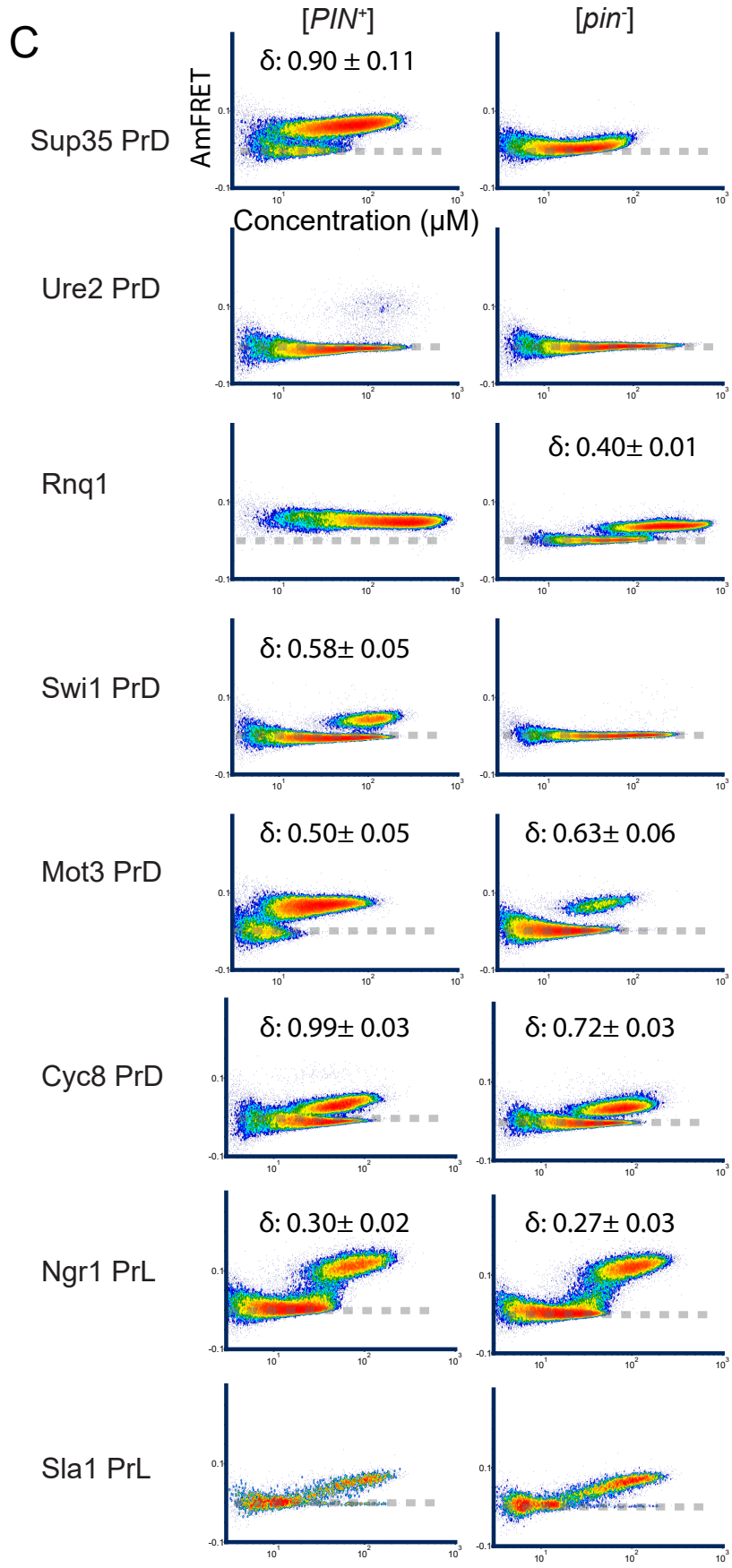
C
[PIN+]
[pin-]
Sup35 PrD
δ: 0.90 ± 0.11
AmFRET
Concentration (μM)
Ure2 PrD
Rnq1
δ: 0.40± 0.01
Swi1 PrD
δ: 0.58± 0.05
Mot3 PrD
δ: 0.50± 0.05
δ: 0.63± 0.06
Cyc8 PrD
δ: 0.99± 0.03
δ: 0.72± 0.03
Ngr1 PrL
δ: 0.30± 0.02
δ: 0.27± 0.03
Sla1 PrL

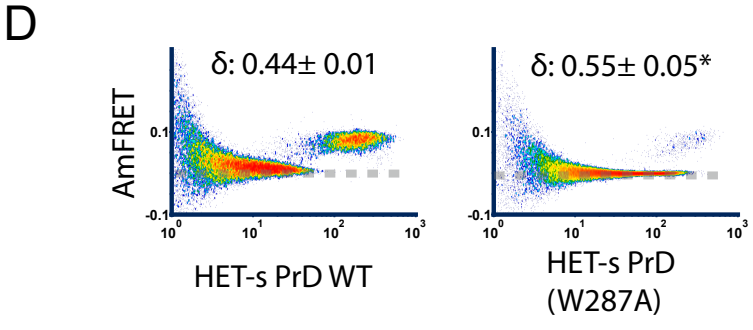
D
δ: 0.44± 0.01
δ: 0.55± 0.05*
AmFRET
HET-s PrD WT
HET-s PrD
(W287A)

Figure S3. Additional characterization of prion and prion-like proteins, related to Fig. 3.

(A) Images of cells acquired by imaging flow cytometry. The cells were selected from high or low-AmFRET populations within the same concentration range, expressing the indicated protein from (A). Representative images for each population are shown. BF, Bright Field.
(B) Representative images showing ThT-stained cells expressing Sla1 PrL or Ngr1 PrL.
(C) DAmFRET plots of known yeast prion-forming sequences and of Ngr1 PrL and Sla1 PrL.
(D) DAmFRET of the PrD of a well-characterized fungal prion HET-s and its known hypomorphic mutant W287A. The inset shows δ± error. *The δ value for W287A is likely underestimated due to the Weibull function necessitating that the high AmFRET fraction goes to 1.

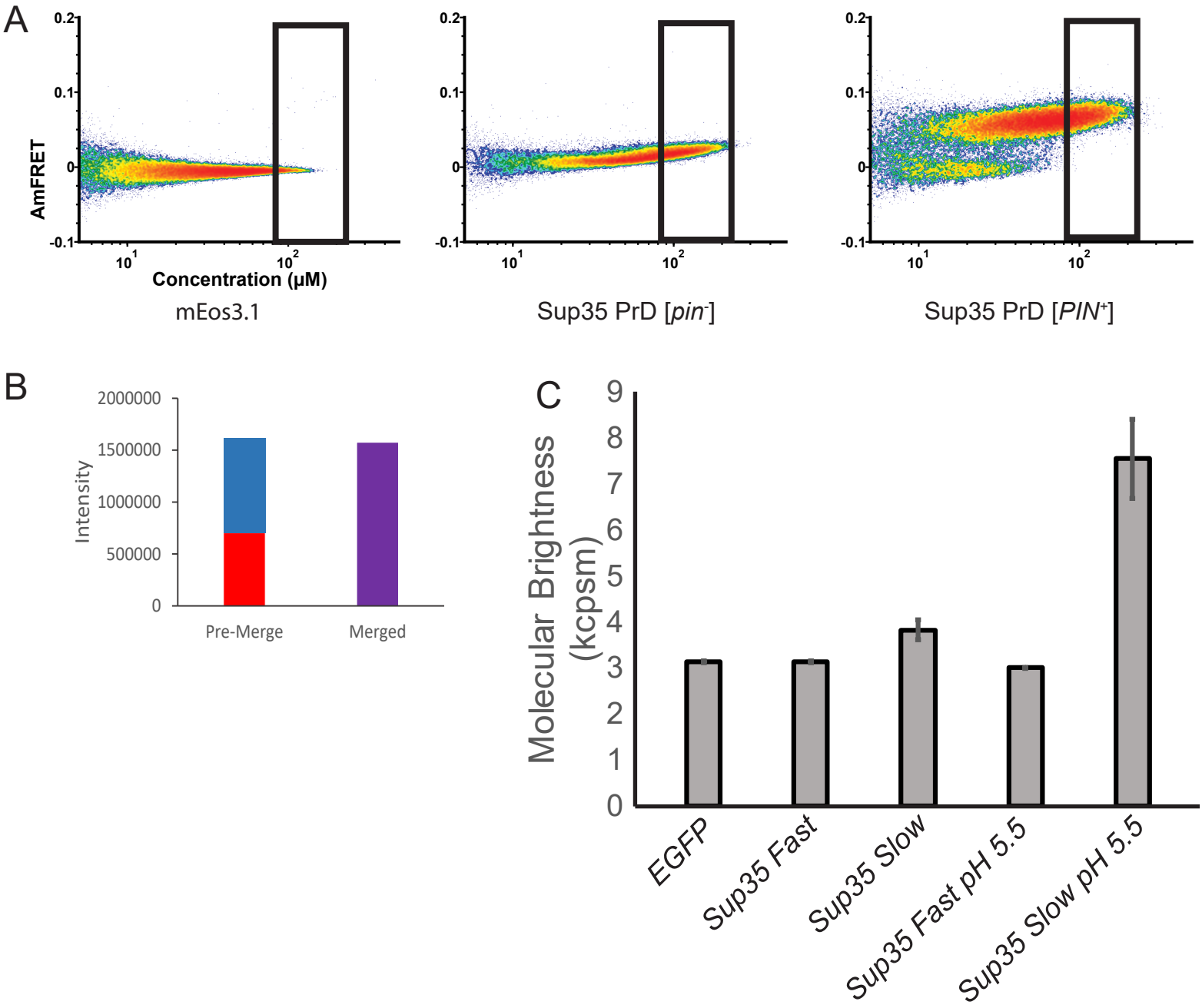

Figure S4. Additional characterization of Sup35 PrD liquid droplets, related to Fig. 4.

(A) DAmFRET plots and the indicated gates used for the quantification of mean AmFRET shown in Fig. 4A.
(B) Intensity (arbitrary units) of the two puncta indicated by arrows in Fig. 4E immediately before (red and blue bar) and after (purple bar) coalescing with each other.
(C) Bar graphs depicting the quantification of FCS, with the molecular brightness of GFP in cells expressing 1x GFP or endogenous, full-length Sup35 fused to GFP. See Methods for details.

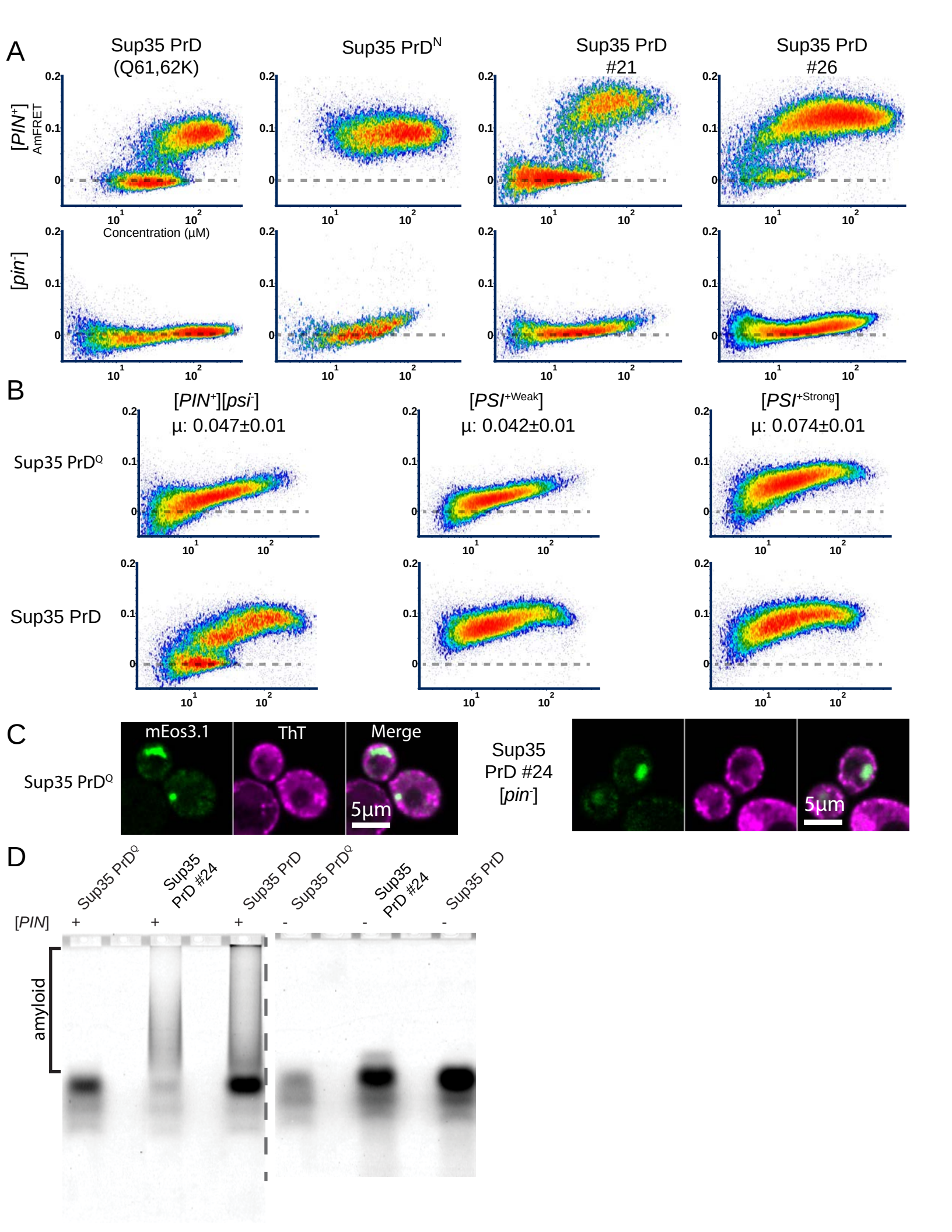
A
Sup35 PrD (Q61,62K)
Sup35 PrD^N
Sup35 PrD #21
Sup35 PrD #26
[PIN+] AmFRET
[pin-]
Concentration (μM)
B
[PIN+][psi-]
μ: 0.047±0.01
[PSI+Weak]
μ: 0.042±0.01
[PSI+Strong]
μ: 0.074±0.01
Sup35 PrD^Q
Sup35 PrD
C
Sup35 PrD^Q
mEos3.1
ThT
Merge
5μm
Sup35 PrD #24 [pin-]
5μm
D
Sup35 PrD^Q
Sup35 PrD #24
Sup35 PrD
Sup35 PrD^Q
Sup35 PrD #24
Sup35 PrD
[PIN]
+ + + - - -
amyloid

Figure S5. Additional characterization of Sup35 PrD variants, related to Fig. 5.

(A) DAmFRET plots of Sup35 PrD mutants and scrambled variants, as an extension of those shown in Fig. 5A.
(B) DAmFRET of Sup35 PrDQ in cells with different endogenous amyloid templates ([PIN^+], [PSI^+weak], or [PSI^+strong]) in comparison with that of Sup35 PrD WT. Mean AmFRET values are denoted as μ.
(C) Representative confocal images depicting ThT staining in cells expressing Sup35 PrDQ or Sup35 PrD #24.
(D) SDD-AGE of Sup35 PrD #24 and Sup35 PrDQ expressed in [PIN^+] or [pin^-] cells, along with WT Sup35 PrD as a positive and negative control for amyloid. The dashed line indicates the two adjacent lanes shown are spliced from different positions in the gel. Alternate lanes were intentionally left blank.

Movie S1. Time-lapse microscopy of cells expressing ASC-mEos3.1, related to Fig. 1E.

Movie S2. Time-lapse microscopy of Sup35 PrD-mEos3.1-expressing cells in the absence of stress, related to Fig. 4F.

Movie S3. Time-lapse microscopy of Sup35 PrD-mEos3.1-expressing cells treated with $NaAsO_2$, related to Fig. 4F.

Movie S4. Time-lapse microscopy of Sup35 PrD-mEos3.1-expressing cells treated with antimycin + 2-deoxyglucose, related to Fig. 4F.

Table S1. Parameters of fits from DAmFRET datasets, related to figures 1-6.

experiment	protein	yeast strain	EC_{50} (μM)	EC_{50} SE	C_{min} (μM)	C_{min} SE	δ	δ SE
[PIN^+] isoforms	Sup35 PrD	rhy1967‡ [PIN^{+High}]	22.9	0.17	1.67	0.46	0.74	0.02
	Sup35 PrD	rhy1966‡ [PIN^{+Med}]	8.92	0.05	3.06	0.24	1.04	0.04
	Sup35 PrD	rhy1965‡ [PIN^{+Low}]	2.33	0.16	1.78	0.38	1.59	0.23
[PIN^+] cross-seeding	Sup35 PrD	rhy1713	13.25	0.33	0.00	1.59	0.90	0.11
	Sup35 PrD*	rhy1852	N/D	N/D	N/D	N/D	N/D	N/D
	Ure2 PrD*	rhy1713	N/D	N/D	N/D	N/D	N/D	N/D
	Ure2 PrD*	rhy1852	N/D	N/D	N/D	N/D	N/D	N/D
	Mot3 PrD	rhy1713	8.66	0.07	1.17	0.66	0.50	0.05
	Mot3 PrD	rhy1852	43.47	0.63	13.59	2.15	0.63	0.06
	Swi1 PrD	rhy1713	104.96	1.39	15.22	5.74	0.58	0.05
	Swi1 PrD*	rhy1852	N/D	N/D	N/D	N/D	N/D	N/D
	Cyc8 PrD	rhy1713	38.20	0.36	0.00	0.69	0.99	0.03
	Cyc8 PrD	rhy1852	50.10	0.31	3.17	1.09	0.72	0.02
	Ngr1 PrL	rhy1713	39.08	0.10	3.36	1.90	0.30	0.02
	Ngr1 PrL	rhy1852	45.49	0.20	1.65	2.91	0.27	0.03
	Rnq1*	rhy1713	N/D	N/D	N/D	N/D	N/D	N/D
	Rnq1	rhy1852	88.01	1.69	0.00	9.48	0.40	0.07
	ASC	rhy1713	23.70	0.09	1.24	0.80	0.38	0.02
	HET-s PrD	rhy1713	33.41	1.10	3.41	0.75	0.44	0.01
	HET-s PrD (W287A)	rhy1713	162.00	6.70	13.00	2.90	0.55	0.05
	sesA	rhy1713	249.00	0.85	0.00	2.16	0.49	0.01
Sup35 PrD mutants	WT	YJW1178‡	18.48	0.52	0.00	1.08	0.67	0.09
	Y46K+Q47K	YJW1178‡	99.38	0.93	99.38	0.93	0.54	0.03
	Q61K+Q62K	YJW1178‡	51.12	1.64	51.12	1.64	0.42	0.18
Sup35 PrD scrambles	WT	rhy1713	14.00	0.12	4.45	0.19	1.04	0.03
	#21	rhy1713	24.20	0.11	5.13	0.19	0.82	0.01
	#24†	rhy1713	N/D	N/D	N/D	N/D	N/D	N/D
	#25*	rhy1713	N/D	N/D	N/D	N/D	N/D	N/D
	#26	rhy1713	8.4	0.0596	2.5	0.1596	1.266	0.03
	PrD^N	rhy1713	N/D	N/D	N/D	N/D	N/D	N/D
	PrD^Q	rhy1713	N/D	N/D	N/D	N/D	N/D	N/D

* exceeded sensitivity of assay
‡ not cell cycle-arrested
† multimodal

Table S2. Plasmids and polypeptide sequences used in this study, related to STAR Methods.

vector	derived plasmid	insert	fusion protein sequence
V08 (encodes linker + mEos3.1 at C-terminus of insert)	rhx1111	sesA	MSEATVSELISSTIKSLEEGIRCHKDVEDDNGLREAFHEAGRGLSVVNQALQAAQGNSAREPQSAMN PLRVCNTKANISASIFKAVAQAPKTSRFEGYKEAVRQEGNGQTVEVLVVGMMKDVCALAENFAIQDQ VKKLHETIEKLSAMKPSLPKEGPGHTFTNIGNGNQYNATDGPQNINQGGNQVTGGTFPGTVNFGSPW PQNPPFEHRNGAEAAAREAAAREAAAREAAAREAAARINMSAIKPDMKIKLRMEGNVNGHHFVIDGDGTGKP FEGKQSMDLEVKEGGPLPFAFDILTTAFHYGNRVFAKYPDNIQDYFKQSFPKGYSWERSLTFEDGGIC NARNDITMEGDTFYNKVRFYGTNFPANGPVMQKKTLKWEPSTEKMYVRDGVLTGDVEMALLLEGNA HYRCDFRTTYKAKEKGVKLPGAHFVDHCIEILSHDKDYNKVKLYEHAVAHSGLPDNARR
BB5b (encodes linker + mEos3.1 at C-terminus of insert)	rhx0927	ASC	MSGRARDAILDALENLTAEELKKFKLKLLSVPLREGYGRIPRGALLSMDALDLTDKLVSFYLETYGAELT ANVLRDMGLQEMAGQLQAATHQGSGAAPAGIQAPPQSAAKPGLHFIDQHRAALIARVTNVEWLLDAL YGKVLTDEQYQAVRAEPTNPSKMRKLFSFTPAWNWTCKDLLLQALRESQSYLVEDLERSGAEAAAR EAAAREAAAREAAARINMSAIKPDMKIKLRMEGNVNGHHFVIDGDGTGKPFEGKQSMDLEVKEGGPL PFAFDILTTAFHYGNRVFAKYPDNIQDYFKQSFPKGYSWERSLTFEDGGICNARNDITMEGDTFYNKVR FYGTNFPANGPVMQKKTLKWEPSTEKMYVRDGVLTGDVEMALLLEGNAHYRCDFRTTYKAKEKGVK LPGAHFVDHCIEILSHDKDYNKVKLYEHAVAHSGLPDNARR
	rhx0935	mEos3.1	MSAIKPDMKIKLRMEGNVNGHHFVIDGDGTGKPFEGKQSMDLEVKEGGPLPFAFDILTTAFHYGNRVF AKYPDNIQDYFKQSFPKGYSWERSLTFEDGGICNARNDITMEGDTFYNKVRFYGTNFPANGPVMQKK TLKWEPSTEKMYVRDGVLTGDVEMALLLEGNAHYRCDFRTTYKAKEKGVKLPGAHFVDHCIEILSHDK DYNKVKLYEHAVAHSGLPDNARR
	rhx0952	HETs PrD	MSKIDAIVGRNSAKDIRTEERARVQLGNVVTAAALHGGIRISDQTTNSVETVVGKGESRVLIGNEYGGK GFWDNNPAFLYKVVMGCRNSISSSPEAAAREAAAREAAAREAAARGGGRINGGGGGAMSAIKPDM KIKLRMEGNVNGHHFVIDGDGTGKPFEGKQSMDLEVKEGGPLPFAFDILTTAFHYGNRVFAKYPDNIQ DYFKQSFPKGYSWERSLTFEDGGICNARNDITMEGDTFYNKVRFYGTNFPANGPVMQKKTLKWEPST EKMYVRDGVLTGDVEMALLLEGNAHYRCDFRTTYKAKEKGVKLPGAHFVDHCIEILSHDKDYNKVKLY EHAVAHSGLPDNARR
	rhx1543	HETs PrD(W287A)	MSKIDAIVGRNSAKDIRTEERARVQLGNVVTAAALHGGIRISDQTTNSVETVVGKGESRVLIGNEYGGK GFADNNPAFLYKVVMGCRNSISSSPEAAAREAAAREAAAREAAARGGGRINGGGGGAMSAIKPDMK IKLRMEGNVNGHHFVIDGDGTGKPFEGKQSMDLEVKEGGPLPFAFDILTTAFHYGNRVFAKYPDNIQD YFKQSFPKGYSWERSLTFEDGGICNARNDITMEGDTFYNKVRFYGTNFPANGPVMQKKTLKWEPSTE KMYVRDGVLTGDVEMALLLEGNAHYRCDFRTTYKAKEKGVKLPGAHFVDHCIEILSHDKDYNKVKLYE HAVAHSGLPDNARR
	rhx0974	SUP35 PrD	MSDSNQGNNQQNYQQYSQNGNQQQGNNRYQGYQAYNAQAQPAGGYYQNYQGYSGYQQGGYQQ YNPDAGYQQQYNPQGGYQQYNPQGGYQQQFNPQGGRGNYKNFNYNNNLQGYQAGFQPQSQGM SLNDFQKQQKQCDPAFLYKVVMGCRNSISSSPEAAAREAAAREAAAREAAARGGGRINGGGGGAM SAIKPDMKIKLRMEGNVNGHHFVIDGDGTGKPFEGKQSMDLEVKEGGPLPFAFDILTTAFHYGNRVFA KYPDNIQDYFKQSFPKGYSWERSLTFEDGGICNARNDITMEGDTFYNKVRFYGTNFPANGPVMQKKT LKWEPSTEKMYVRDGVLTGDVEMALLLEGNAHYRCDFRTTYKAKEKGVKLPGAHFVDHCIEILSHDKD YNKVKLYEHAVAHSGLPDNARR
	rhx1500	SUP35 PrD(Q61K,Q62K)	MSDSNQGNNQQNYQQYSQNGNQQQGNNRYQGYQAYNAQAQPAGGYYQNYQGYSGYQQGGYKK YNPDAGYQQQYNPQGGYQQYNPQGGYQQQFNPQGGRGNYKNFNYNNNLQGYQAGFQPQSQGM SLNDFQKQQKQCDPAFLYKVVMGCRNSISSSPEAAAREAAAREAAAREAAARGGGRINGGGGGAM SAIKPDMKIKLRMEGNVNGHHFVIDGDGTGKPFEGKQSMDLEVKEGGPLPFAFDILTTAFHYGNRVFA KYPDNIQDYFKQSFPKGYSWERSLTFEDGGICNARNDITMEGDTFYNKVRFYGTNFPANGPVMQKKT LKWEPSTEKMYVRDGVLTGDVEMALLLEGNAHYRCDFRTTYKAKEKGVKLPGAHFVDHCIEILSHDKD YNKVKLYEHAVAHSGLPDNARR
	rhx1499	SUP35 PrD(Y46K,Q47K)	MSDSNQGNNQQNYQQYSQNGNQQQGNNRYQGYQAYNAQAQPAGGYKKNYQGYSGYQQGGYQQ YNPDAGYQQQYNPQGGYQQYNPQGGYQQQFNPQGGRGNYKNFNYNNNLQGYQAGFQPQSQGM SLNDFQKQQKQCDPAFLYKVVMGCRNSISSSPEAAAREAAAREAAAREAAARGGGRINGGGGGAM SAIKPDMKIKLRMEGNVNGHHFVIDGDGTGKPFEGKQSMDLEVKEGGPLPFAFDILTTAFHYGNRVFA KYPDNIQDYFKQSFPKGYSWERSLTFEDGGICNARNDITMEGDTFYNKVRFYGTNFPANGPVMQKKT LKWEPSTEKMYVRDGVLTGDVEMALLLEGNAHYRCDFRTTYKAKEKGVKLPGAHFVDHCIEILSHDKD YNKVKLYEHAVAHSGLPDNARR
	rhx1305	SUP35 PrD(N)	MSDSNNGNNNNNYNNYSNNGNNNNGNNRYNGYNAYNANANPAGGYYNNYNGYSGYNNGGYNNYN PDAGYNNNYNPNGGYNNYNPNGGYNNNFNPNGGRGNYKNFNYNNNLNGYNAGFNPNSNGMSLND FNKNNKNAAPKPKKTLKLVSSSGIKLANATKKVGTKPAESDKKEEEKSAETKEPTKEPTKVEEPVKKE EKPVQTEEKTEEKSELPKVEDLKISESTHNTNNANVTSADALIKEQEEEVDDEVVNDNPAFLYKVVMG CRNSISSSPEAAAREAAAREAAAREAAARGGGRINGGGGGAMSAIKPDMKIKLRMEGNVNGHHFVID GDGTGKPFEGKQSMDLEVKEGGPLPFAFDILTTAFHYGNRVFAKYPDNIQDYFKQSFPKGYSWERSL TFEDGGICNARNDITMEGDTFYNKVRFYGTNFPANGPVMQKKTLKWEPSTEKMYVRDGVLTGDVEMA LLLEGNAHYRCDFRTTYKAKEKGVKLPGAHFVDHCIEILSHDKDYNKVKLYEHAVAHSGLPDNARR

Table S2 (cont). Plasmids and polypeptide sequences used in this study, related to STAR Methods.

vector	derived plasmid	insert	fusion protein sequence
BB5b (encodes linker + mEos3.1 at C-terminus of insert)	rhx1306	SUP35 PrD(Q)	MSDSQQGQQQQQYQQYSQQGQQQQGQQRYQGYQAYQAQAQPAGGYYQQYQGYSGYQQGGYQ QYQPDAGYQQQYQPQGGYQQYQPQGGYQQQFQPQGGRGQYKQFQYQQQLQGYQAGFQPQSQ GMSLQDFQKQQKQAAPKPKKTLKLVSSSGIKLANATKKVGTKPAESDKKEEEKSAETKEPTKEPTKV EEPVKKEEKPVQTEEKTEEKSELPKVEDLKISESTHNTNNANVTSADALIKEQEEEVDDEVVNDNPAF LYKVVMGCRNSISSSPEAAAREAAAREAAAREAAARGGGRINGGGGGAMSAIKPDMKIKLRMEGNV NGHHFVIDGDGTGKPFEGKQSMDLEVKEGGPLPFAFDILTTAFHYGNRVFAKYPDNIQDYFKQSFPKG YSWERSLTFEDGGICNARNDITMEGDTFYNKVRFYGTNFPANGPVMQKKTLKWEPSTEKMYVRDGV LTGDVEMALLLEGNAHYRCDFRTTYKAKEKGVKLPGAHFVDHCIEILSHDKDYNKVKLYEHAVAHSGL PDNARR
	rhx1590	SUP35 PrD(#25)	MSSAQQKNNQAGQQQNQPQQGYGSNRQQYQNSQQPYYGGNGYYQGQYPGGGYFYQGNNNQNQ PFQQNPDLYGQGQYGYAGYNYGNNANANGQQNQDGGYYQYNNYQQYNQQQRYAGFQPQSQGM SLNDFQKQQKQCDPAFLYKVVMGCRNSISSSPEAAAREAAAREAAAREAAARGGGRINGGGGGAM SAIKPDMKIKLRMEGNVNGHHFVIDGDGTGKPFEGKQSMDLEVKEGGPLPFAFDILTTAFHYGNRVFA KYPDNIQDYFKQSFPKGYSWERSLTFEDGGICNARNDITMEGDTFYNKVRFYGTNFPANGPVMQKKT LKWEPSTEKMYVRDGVLTGDVEMALLLEGNAHYRCDFRTTYKAKEKGVKLPGAHFVDHCIEILSHDKD YNKVKLYEHAVAHSGLPDNARR
	rhx1592	SUP35 PrD(#21)	MSQYNSYNGQQQQFQNNQYQGNRDQQGYSGYQGDAYNQQGQYYPQGNGPNYYNYGNQGYKNQ QAGQQGGYANNGFNGLNYRYGPQYQGYYNYNQGQPPQNAYQAQQQGQQNQSNAGFQPQSQGM SLNDFQKQQKQCDPAFLYKVVMGCRNSISSSPEAAAREAAAREAAAREAAARGGGRINGGGGGAM SAIKPDMKIKLRMEGNVNGHHFVIDGDGTGKPFEGKQSMDLEVKEGGPLPFAFDILTTAFHYGNRVFA KYPDNIQDYFKQSFPKGYSWERSLTFEDGGICNARNDITMEGDTFYNKVRFYGTNFPANGPVMQKKT LKWEPSTEKMYVRDGVLTGDVEMALLLEGNAHYRCDFRTTYKAKEKGVKLPGAHFVDHCIEILSHDKD YNKVKLYEHAVAHSGLPDNARR
	rhx1589	SUP35 PrD(#26)	MSYQYQNNYGNQGNQGQQYNNYSQGGAQPQLQRYQYQQPYPQYYYGNQNQQYYQQYQPQQYG GANYRGQNQNFYGNDQYAGQYGGGNNNNGSGDQGNSNAKPQGQQNGQFNQYAAGFQPQSQGM SLNDFQKQQKQCDPAFLYKVVMGCRNSISSSPEAAAREAAAREAAAREAAARGGGRINGGGGGAM SAIKPDMKIKLRMEGNVNGHHFVIDGDGTGKPFEGKQSMDLEVKEGGPLPFAFDILTTAFHYGNRVFA KYPDNIQDYFKQSFPKGYSWERSLTFEDGGICNARNDITMEGDTFYNKVRFYGTNFPANGPVMQKKT LKWEPSTEKMYVRDGVLTGDVEMALLLEGNAHYRCDFRTTYKAKEKGVKLPGAHFVDHCIEILSHDKD YNKVKLYEHAVAHSGLPDNARR
	rhx1591	SUP35 PrD(#24)	MSNNQNGQPNNPYRQNGQQYYYNPQNSYGANGQQNRYGYYQNQYYQQAGGSNQFGNQGYDKN GYQYQFQQAQYQNQLYQGYANNGNSGQQNAGNPYGGGGYQDQQQGQQYYQQPAGFQPQSQGM SLNDFQKQQKQCDPAFLYKVVMGCRNSISSSPEAAAREAAAREAAAREAAARGGGRINGGGGGAM SAIKPDMKIKLRMEGNVNGHHFVIDGDGTGKPFEGKQSMDLEVKEGGPLPFAFDILTTAFHYGNRVFA KYPDNIQDYFKQSFPKGYSWERSLTFEDGGICNARNDITMEGDTFYNKVRFYGTNFPANGPVMQKKT LKWEPSTEKMYVRDGVLTGDVEMALLLEGNAHYRCDFRTTYKAKEKGVKLPGAHFVDHCIEILSHDKD YNKVKLYEHAVAHSGLPDNARR
	rhx0578	URE2 PrD	MMNNNGNQVSNLSNALRQVNIGNRNSNTTTDQSNINFEFSTGVNNNNNNNSSSNNNNVQNNNSGRN GSQNNDNENNIKNTLEQHRQQQQCDPAFLYKVVMGCRNSISSSPEAAAREAAAREAAAREAAARGG GRSLGGGGGAMSAIKPDMKIKLRMEGNVNGHHFVIDGDGTGKPFEGKQSMDLEVKEGGPLPFAFDIL TTAFHYGNRVFAKYPDNIQDYFKQSFPKGYSWERSLTFEDGGICNARNDITMEGDTFYNKVRFYGTNF PANGPVMQKKTLKWEPSTEKMYVRDGVLTGDVEMALLLEGNAHYRCDFRTTYKAKEKGVKLPGAHF VDHCIEILSHDKDYNKVKLYEHAVAHSGLPDNARR
	rhx0950	MOT3 PrD	MNADHHLQQQQQQRQQHQQQQHQQQQHQHQHQQQQHTILQNVSNTNNIGSDSLASQPFNTTTVSS NKDDVMVNSGARELPMPLHQQQYIYPYYQYTSNNSNNNNVTAGNNMSASPIVHNNSNNSNNSNISAS DYTVANNSTSNNNNNNNNNNNNNNNNIHPNQFTAAANMNSNAAAAAYYSFPTANMPIPQQDQQYMFN PASYISHYYSAVNSNNNGNNAANNGSNNSSHSAPAPAPGPPHHHHHHSNTHNNLNNGGAVNTNNAP QHHPTIITDQFQFQLQQNPSPNLNLNINPAQCDPAFLYKVVMGCRNSISSSPEAAAREAAAREAAARE AAARGGGRINGGGGGAMSAIKPDMKIKLRMEGNVNGHHFVIDGDGTGKPFEGKQSMDLEVKEGGPL PFAFDILTTAFHYGNRVFAKYPDNIQDYFKQSFPKGYSWERSLTFEDGGICNARNDITMEGDTFYNKVR FYGTNFPANGPVMQKKTLKWEPSTEKMYVRDGVLTGDVEMALLLEGNAHYRCDFRTTYKAKEKGVK LPGAHFVDHCIEILSHDKDYNKVKLYEHAVAHSGLPDNARR
	rhx1409	SWI1 PrD	MDFFNLNNNNNNNNTTTTTTTTNNNNTNNNNTNNNNNPANNTNNNNSTGHSSNTNNNTNNNNTNTGAS GVDDFQNFFDPKPFDQNLDSNNNNSNSNNNDNNNSNTVASSTNFTSPTAVVNNAAPANVTGGKAAN FIQNQSPQFNSPYDSNNSNTNLNSLSPQAILAKNSIIDSSNLPLQAQQQLYGGNNNNNSTGIANDNVITP HFITNVQSISQNSSSSTPNTNSNSTPNANQQFLPFNNSASNNGNLTSNQLISNYAASNSMDRSSSASN EFVPNTSDNNNNSNNHNMRNNSNNKTSNNNNVTAVPAATPANTNNSTSNANTVFSERAAMFAALQQ KQQQRFQALQQQQQQQQNQQQQNQQPQRQRQQQQCDPAFLYKVVMGCRNSISSSPEAAAREAA AREAAAREAAARGGGRINGGGGGAMSAIKPDMKIKLRMEGNVNGHHFVIDGDGTGKPFEGKQSMDL EVKEGGPLPFAFDILTTAFHYGNRVFAKYPDNIQDYFKQSFPKGYSWERSLTFEDGGICNARNDITME GDTFYNKVRFYGTNFPANGPVMQKKTLKWEPSTEKMYVRDGVLTGDVEMALLLEGNAHYRCDFRTT YKAKEKGVKLPGAHFVDHCIEILSHDKDYNKVKLYEHAVAHSGLPDNARR

Table S2 (cont). Plasmids and polypeptide sequences used in this study, related to STAR Methods.

vector	derived plasmid	insert	fusion protein sequence
BB5b (encodes linker + mEos3.1 at C-terminus of insert)	rhx1392b	CYC8 PrD	MSQPNDQGNPLNTRISAQSANATASMVQQQHPAQQTPINSSATMYSNGASPQLQAQAQAQAQA QAQAQAQAQAQAQAQAQAQAQAQAQAQAQAHAQAQAQAQAQAQAQAQAQQQQQQQQ QQQQQQQQQQQQQQQQQQQQQQQLQPLPRQQLQQKGVSVQMLNPQQGQPYITQPTVIQAHQLQPF STQAMEHPQSSQLPPQQQQLQSVQHPQQLQGQPQAQAPQPLIQHNVEQNCDPAFLYKVVMGCRN SISSSPEAAAREAAAREAAAREAAARGGGRINGGGGGAMSAIKPDMKIKLRMEGNVNGHHFVIDGDG TGKPFEGKQSMDLEVKEGGPLPFAFDILTTAFHYGNRVFAKYPDNIQDYFKQSFPKGYSWERSLTFE DGGICNARNDITMEGDTFYNKVRFYGTNFPANGPVMQKKTLKWEPSTEKMYVRDGVLTGDVEMALLL EGNAHYRCDFRTTYKAKEKGVKLPGAHFVDHCIEILSHDKDYNKVKLYEHAVAHSGLPDNARR
	rhx1469	NGR1 PrL	MSQQQQQQDGNFSMEQMAHNNYYNYNNYDYHRNKNGSHSDLVNLQRSNVPYMQEDGALYPHQ YSSPSYSLHPTGNQFSNATNNLPQFGNAMSISMQLPNGNSNKTASSMNTNPNTNMIMNSNMNMNMN VNPVPYGMGNGANMYCDPAFLYKVVMGCRNSISSSPEAAAREAAAREAAAREAAARGGGRINGGG GGAMSAIKPDMKIKLRMEGNVNGHHFVIDGDGTGKPFEGKQSMDLEVKEGGPLPFAFDILTTAFHYGN RVFAKYPDNIQDYFKQSFPKGYSWERSLTFEDGGICNARNDITMEGDTFYNKVRFYGTNFPANGPVM QKKTLKWEPSTEKMYVRDGVLTGDVEMALLLEGNAHYRCDFRTTYKAKEKGVKLPGAHFVDHCIEILS HDKDYNKVKLYEHAVAHSGLPDNARR
	rhx1456	SLA1 PrL	MCGGAQFPQTSFNVQGQQQLPTGSILPVQKTANGLISANTGVSMPTVQRTGGTMIPQTSFGVSQQLT GGAMMTQPQNTGSAMMPQTSFNAVPQITGGAMMPQTSFNALPQVTGGAMMPLQRTGGALNTFNTG GAMIPQTSFSSQAQNTGGFRPQSQFGLTLQKTGGIAPLNQNQFTGGAMNTLSTGGVLQQQQPQTMNT FNTGGVMQELQMMTTFNTGGAMQQPQMMNTFNTDGIMQQPQMMNTFNTGGAMQQPQQQALQNQP TGFGFGNGPQQSRQANIFNATASNPFGFDPAFLYKVVMGCRNSISSSPEAAAREAAAREAAAREAA ARGGGRINGGGGGAMSAIKPDMKIKLRMEGNVNGHHFVIDGDGTGKPFEGKQSMDLEVKEGGPLPF AFDILTTAFHYGNRVFAKYPDNIQDYFKQSFPKGYSWERSLTFEDGGICNARNDITMEGDTFYNKVRFY GTNFPANGPVMQKKTLKWEPSTEKMYVRDGVLTGDVEMALLLEGNAHYRCDFRTTYKAKEKGVKLP GAHFVDHCIEILSHDKDYNKVKLYEHAVAHSGLPDNARR
CA (encodes mEos3.1 + linker at N-terminus of insert)	rhx1879	RNQ1	MSAIKPDMKIKLRMEGNVNGHHFVIDGDGTGKPFEGKQSMDLEVKEGGPLPFAFDILTTAFHYGNRVF AKYPDNIQDYFKQSFPKGYSWERSLTFEDGGICNARNDITMEGDTFYNKVRFYGTNFPANGPVMQKK TLKWEPSTEKMYVRDGVLTGDVEMALLLEGNAHYRCDFRTTYKAKEKGVKLPGAHFVDHCIEILSHDK DYNKVKLYEHAVAHSGLPDNARRGAPEAAAREAAAREAAAREAAARTSLYKKAGYMDTDKLISEAE SHFSQGNHAEAVAKLTSAAQSNPNDEQMSTIESLIQKIAGYVMDNRSGGSDASQDRAAGGGSSFMN TLMADSKGSSQTQLGKLALLATVMTHSSNKGSSNRGFDVGTVMSMLSGSGGGSQSMGASGLAALA SQFFKSGNNSQGQGQGQGQGQGQGQGQGQGSFTALASLASSFMNSNNNNQQGQNQSSGGSSFG ALASMASSFMHSNNNQNSNNSQQGYNQSYQNGNQNSQGYNNQQYQGGNGGYQQQQGQSGGAF SSLASMAQSYLGGGQTQSNQQQYNQQGQNNQQQYQQQGQNYQHQQQGQQQQQGHSSSFSALA SMASSYLGNNSNSNSSYGGQQQANEYGRPQQNGQQQSNEYGRPQYGGNQNSNGQHESFNFSGN FSQQNNNGNQNRY

Table S3. Yeast strains used in this study, related to STAR Methods.

yeast strain	background	genotype	plasmotype	parent strain, source
Y7092	S288c	MATα lyp1Δ can1Δ::STE2pr_SpHIS5 his3Δ1 leu2Δ0 ura3Δ0 met15Δ0	[*PIN*$^{+}$]	Tong and Boone 2007
rhy1851	S288c	MATα lyp1Δ can1Δ::STE2pr_SpHIS5 his3Δ1 leu2Δ0 ura3Δ0 met15Δ0	[*pin*$^{-}$]	Y7092, this study
rhy1713	S288c	MATα lyp1Δ can1Δ::STE2pr_SpHIS5 his3Δ1 leu2Δ0 ura3Δ0 met15Δ0 cln3Δ0::GAL1pr_WHI5_hphMX	[*PIN*$^{+}$]	Y7092, this study
rhy1852	S288c	MATα lyp1Δ can1Δ::STE2pr_SpHIS5 his3Δ1 leu2Δ0 ura3Δ0 met15Δ0 cln3Δ0::GAL1pr_WHI5_hphMX	[*pin*$^{-}$]	yrh1713, this study
L2910	74-D694	MATa ade1-14 leu2-3,112 his3Δ200 trp1-289 ura3-52	[*pin*$^{-}$]	Bradley et al. 2002
L1943	74-D694	MATa trp1-1 ura3-1 leu2-3,112 his3-11,15 ade2-1 can1-100 met2Δ1 lys2Δ2	low [*PIN*$^{+}$]	Bradley et al. 2002
L1945	74-D694	MATa ade1-14 leu2-3,112 his3Δ200 trp1-289 ura3-52	medium [*PIN*$^{+}$]	Bradley et al. 2002
L1749	74-D694	MATa ade1-14 leu2-3,112 his3Δ200 trp1-289 ura3-52	high [*PIN*$^{+}$]	Bradley et al. 2002
YJW1178	74-D694	MATa ade1-14 leu2-3,112 his3Δ200 trp1-289 ura3-52	[*PIN*$^{+}$] [*psi*$^{-}$]	Tanaka et al. 2006
YJW1180	74-D694	MATa ade1-14 leu2-3,112 his3Δ200 trp1-289 ura3-52	[*PIN*$^{+}$] [*PSI*$^{+\text{strong}}$]	Tanaka et al. 2006
YJW1181	74-D694	MATa ade1-14 leu2-3,112 his3Δ200 trp1-289 ura3-52	[*PIN*$^{+}$] [*PSI*$^{+\text{weak}}$]	Tanaka et al. 2006
rhy1965	S288c/74-D694	MATa/α lyp1Δ/LYP1 can1Δ::STE2pr_SpHIS5/can1-100 his3Δ1/his3-11,15 leu2Δ0/leu2-3,112 ura3Δ0/ura3-1 met15Δ0/MET15 trp1-1/TRP1 ade2-1/ADE2 met2Δ1/MET2 lys2Δ2/LYS2	low [*PIN*$^{+}$]	yrh1851 X L1943, this study
rhy1966	S288c/74-D694	MATa/α lyp1Δ/LYP1 can1Δ::STE2pr_SpHIS5/can1-100 his3Δ1/his3-11,15 leu2Δ0/leu2-3,112 ura3Δ0/ura3-1 met15Δ0/MET15 trp1-1/TRP1 ade2-1/ADE2 met2Δ1/MET2 lys2Δ2/LYS2	medium [*PIN*$^{+}$]	yrh1851 X L1945, this study
rhy1967	S288c/74-D694	MATa/α lyp1Δ/LYP1 can1Δ::STE2pr_SpHIS5/can1-100 his3Δ1/his3-11,15 leu2Δ0/leu2-3,112 ura3Δ0/ura3-1 met15Δ0/MET15 trp1-1/TRP1 ade2-1/ADE2 met2Δ1/MET2 lys2Δ2/LYS2	high [*PIN*$^{+}$]	yrh1851 X L1749, this study

Method S1

Developing a technique to detect nucleation of proteins *in vivo* required a few moving parts to come together. The necessity to acquire single-cell measurements across large cell populations while also determining cytosolic volume and protein localization within each cell led us to imaging flow cytometry as the appropriate platform (Basiji and O'Gorman, 2015).

Ensuring experimental independence of each cell required that we restrict intercellular interactions. We therefore employed the unicellular eukaryote, budding yeast. Notably, yeast cell walls are impermeable to extracellular amyloids and prion-containing exosomes (Kabani and Melki, 2015; King and Diaz-Avalos, 2004) whereas cultured mammalian cells readily internalize these structures (Grassmann et al., 2013). We eliminated the additional possibility of mitotic inheritance of nucleated assemblies by genetically inducing cell cycle arrest during query protein expression (see Fig. 1C and Method Details). In short, every cell of the resulting yeast strain can be considered as an independent, femtoliter-volume vessel for protein assembly. We, therefore, created an *in vivo* system that allows for measurements that have not yet been attempted *in vitro* let alone *in vivo*.

Measuring protein self-assembly requires a sensitive reporter that scales with the order of assembly and one that is reproducible across experiments. Many techniques were considered for the reporter. Förster Resonance Energy Transfer (FRET) occurs between two fluorophores that have overlapping spectra, when in close proximity. FRET is widely used to detect interactions between two corresponding protein species fused to those fluorophores (Jares-Erijman and Jovin, 2003). However, creating the two fusions for each protein, and expressing them to the same ratio in all cells across a range of expression levels, would be exceedingly difficult. We likewise excluded protein complementation and two hybrid assays from consideration. Available approaches that use a single fusion protein to detect self-assembly, such as fluorescence anisotropy and enzyme loss of function assays, were not considered due to their limited dynamic range and throughput.

We reasoned that high-throughput, sensitized emission FRET between complementary fluorophores could be realized if they were both expressed from the same genetic construct. Individual molecules of the fusion protein would have to mature stochastically into one or the other fluorophore, resulting in a mixture of the two at the cellular level. This ensured a consistent ratio of donor to acceptor molecules, regardless of the expression level of the protein. We further reasoned that photoconvertible fluorescent proteins could be employed for this purpose (Wolf et al., 2013). After testing several, we chose to proceed with mEos3.1, a monomeric bright green fluorescent protein that can be converted irreversibly to a bright red fluorescent form upon illumination with violet light (Zhang et al., 2012). Importantly, the emission spectrum of the green form (solid curves) strongly overlaps (shaded in yellow) with the excitation spectrum of the red form (dotted curves), as necessary for FRET to occur (Fig. 1A). The ratio of green to red molecules and thereby the sensitivity of the mixture to self-assembly can be precisely controlled by modulating the intensity and duration of violet light

exposure. We term this approach Amphifluoric FRET (AmFRET) due to the dual nature of the fluorescent moiety.

To detect nucleation barriers, we needed to evaluate the distribution of AmFRET values, or DAmFRET, across a wide range of intracellular protein concentrations. We therefore inducibly expressed mEos3.1 fusion proteins from an episomal plasmid whose copy number varies more than one hundred fold between cells (Fig. 1B; Futcher and Cox, 1984; Loison et al., 1989). After eighteen hours of protein expression (driven by an inducible *GAL1* promoter) in galactose medium, cell cultures were uniformly illuminated with violet light to convert a fraction of mEos3.1 molecules from the green (donor) to the red (acceptor) form (Fig. 1C). We limited the illumination to an empirically optimized dose that yielded maximum FRET intensity. We established that photoconversion efficiency was insensitive to expression level as well as to the identity and structure of the fusion partner (Fig. S1B) and did not vary between cells (Fig. S1C), enabling us to indirectly measure total protein levels as the product of intensity of acceptor fluorescence and an empirically determined molecular brightness and photoconversion factor (see Method Details). We then divided each cell's total protein level by its approximate cytosolic volume as calculated from the bright-field image to derive absolute protein concentrations. We used the ratio of acceptor fluorescence when excited indirectly (at 488 nm) to directly (at 561 nm) to approximate FRET efficiency, and refer to this ratio as simply, "AmFRET".